

Using liquid phase precursor method to create a high-efficiency $\text{Ca}_2\text{SiO}_4:\text{Eu}^{2+}$ green-emitting phosphor

Phuc Dang Huu¹, Dieu An Nguyen Thi²

¹Institute of Applied Technology, Thu Dau Mot University, Binh Duong Province, Binh Duong, Vietnam

²Faculty of Electrical Engineering Technology, Industrial University of Ho Chi Minh City, Ho Chi Minh, Vietnam

Article Info

Article history:

Received Jul 22, 2021

Revised Feb 20, 2022

Accepted Apr 21, 2022

Keywords:

Color homogeneity

Luminous flux

Monte Carlo theory

WLEDs

β -sialon: Eu^{2+}

ABSTRACT

A standard solid-state reaction (SSR), a new fluid phase preparatory method utilizing LPP- $\text{SiO}_2(\text{sol})$, and a water-based soluble silicone compound were employed to manufacture green Eu^{2+} -based Ca_2SiO_4 phosphors liquid phase precursor (LPP-WSS). The generated phosphors feature large excitation spectra in the range of 225–450 nm and a strong green emission reaches the peak value at 502 nm owing to a $4f^65d^1 \rightarrow 4f^7(8S_{7/2})$ transition of Eu^{2+} . These samples burned at 1100 °C produce the highest luminous intensity. The luminous properties of phosphors, which are manufactured by the liquid phase precursor LPP-WSS technique, were investigated at the range of 0.1–5.0 mol percent of Eu^{2+} , with the maximum emission density observed at the value of 3.0 mol percent of Eu^{2+} . The phosphors produced by the LPP-WSS technique exhibited a more uniform phase dispersion and higher luminous strength than those produced using the other procedures, according to a detailed report based on numerous characterizations. As a result, $\text{Ca}_2\text{SiO}_4:\text{Eu}^{2+}$ has an indisputable possibility in white light-emitting diodes WLEDs and fluorescent lighting.

This is an open access article under the [CC BY-SA](https://creativecommons.org/licenses/by-sa/4.0/) license.



Corresponding Author:

Dieu An Nguyen Thi

Faculty of Electrical Engineering Technology, Industrial University of Ho Chi Minh City

No. 12 Nguyen Van Bao Street, Ho Chi Minh City, Vietnam

Email: nguyenthidieuan@iuh.edu.vn

1. INTRODUCTION

Rare-earth doped silicate phosphors have recently received a lot of attention because of their possible use in the white light-emitting diodes (WLEDs) and fluorescent lighting, both of these materials hold promise during the next solid-state lighting generation. The broad photoluminescent spectra, immense chemical stability and heat resistance, and reasonable synthesis cost are all important characteristics of silicate phosphors for many applications [1]-[3]. The divalent europium loaded the alkaline earth silicate phosphor structure is of specific importance because the ion radii of alkaline earth ions, including 0.112 nm of $[\text{Eu}^{2+}]$ and $[\text{Sr}^{2+}]$, 0.099 nm of $[\text{Ca}^{2+}]$, and 0.134 nm of $[\text{Ba}^{2+}]$, are equivalent to those of the divalent europium. Consequently, divalent europium is more stable and diffuses more freely into the lattice sites in an alkaline earth silicate host [4]-[6].

An often-used method to create alkaline silicate phosphors is the solid-state reaction process (SSR) in extreme temperatures over long durations. This SSR method's outputs, on the other hand, have substantial flaws, such as uneven phase dispersion and bulky, non-homogeneous shape of the particle that affect the phosphors' luminous capabilities [7], [8]. The synthesis of alkaline silicate phosphors by hydrothermal means was investigated, however smooth particle shape and a uniform crystalline structure appear to be challenging to achieve using a standard solution technique [9]. A unique liquid phase precursor (LPP) technique has solved these issues. Solution-based synthesis can result in significant reductions in the synthesized heating and timing,

also the improvements in phase compound and uniformity, as an extraordinarily mixing process in extreme degree at the nanoscale is obtained by combining all the ingredients altogether [10]. It is critical to choose an adequate silicon reagent for the LPP technique of creating silicate phosphor. The criteria require not only miscible in water but also reacts quickly. Most silicates are made with tetraethoxysilane (TEOS) or TEOS derivatives, despite the fact that they are inconsistent and insoluble in distilled water [11]-[13]. We previously employed SiO₂ sol with a homogeneous particle diameter of 10 nm to produce silicate phosphors using the LPP method, which we called the LPP-SiO₂(sol) method [14]. Recently, Pang *et al.* [15] developed a new water-dissolvable silicon complex (WSS). TEOS and propylene glycol (PG) were blended then agitated over 48 hours with the temperature of 80 degrees Celsius, then blended with hydrochloric acid HCl solution for an hour with the temperature of 80 degrees Celsius. Lastly, the outcome is a transparent silicon compound solution. After being maintained in an ambient atmosphere for several weeks, this solution was thought to be able to be mixed with distilled water in either concentration without inducing the hydrolysis. The utilization of the WSS chemical within the LPP process is predicted to improve the production of silicate phosphors. As a consequence, this study used the LPP-SiO₂(sol), LPP-WSS, and SSR procedures to manufacture Ca₂SiO₄:Eu²⁺ phosphors at varied fabrication temperatures. According to the findings, the LPP-WSS procedure is the most effective of the three ways. This study also investigates the activator concentration-dependent luminescence features.

2. COMPUTATIONAL SIMULATION

2.1. X-ray diffraction analysis for Ca₂SiO₄:Eu²⁺ phosphor

Although the traditional solution approach may be appealing, the non-uniformity of the raw material has resulted in a multi-stage crystal construction for the silica phosphors produced using the solution technique [16], [17]. Figure 1 shows the LED image used in this study. The samples produced utilizing the LPP-WSS technique had a more uniform crystal structure, based on the current JCPDS card (No. 33-0302). Which may be compared to a Ca₂SiO₄ crystalline phase in the typical β form (monoclinic). The x-ray diffraction XRD figures of the materials generated utilizing the LPP-SiO₂(sol) approach work with the conventional Ca₂SiO₄ β phase (monoclinic) crystallite. Even at a more elevated temperature, however, the crystallinity did not improve noticeably. The phosphor produced using the SSR method had a poor XRD figure with large peaks that were challenging to discern in 1000°C, indicating poor crystallinity nature and small particle size. The conversion from β phase to γ phase occurs when phosphor is created at 1200°C.

The stage consistency of Eu²⁺-doped and pristine Ca₂SiO₄ crystal can assess phase distribution discrepancies distributions in three different techniques of phosphors manufactured. Both the β and γ phases of pure Ca₂SiO₄ crystallite are stable at ambient temperature. The γ phase is frequently formed at a greater temperature compared to the β phase because of its thermodynamically consistent crystalline figure [18], [19]. Only the β phase appears to be stable in the Eu²⁺ doped Ca₂SiO₄ phosphor. As a result, the Eu²⁺ ions in Ca₂SiO₄ at high temperatures can stabilize the β phase [20]. The phase conversion during the SSR procedure is caused by the non-homogeneous dispersion of Eu²⁺ atoms throughout the host matrix. As a consequence of the XRD examination, the LPP approach may create homogeneous single-crystalline phosphor powders, which are difficult to acquire using the SSR method.



Figure 1. Photograph of WLEDs

2.2. The concentration of Eu²⁺ functions as fluorescent properties

The concentration of Eu²⁺ influence on the fluorescent characteristic of the phosphor Ca₂SiO₄:Eu²⁺ is shown in Figure 2. The LPP-WSS technique was used to synthesize all phosphors at 1100°C, which were

then evaluated at room temperature. The light intensity of the phosphors grew with increasing doping concentration when this reached 3.0 mol percent, and after that decreased as the Eu^{2+} concentration increased, a phenomenon known as concentration quenching. It is possible that it is caused by a deep connection among productive ions separated by a slight gap, which is linked to an increase in non-radiational power conversion among the productive ions or among the active ions and the hosting lattice [21]-[23]. Furthermore, when concentrations increased, the gaussian regions correlative magnitude lay at the values of 310 and 400 nm in stimulation spectrum increased higher over the other two regions, reflecting a rise in Eu^{2+} occupancy at smaller Ca(1) sites. However, as the concentration of Eu^{2+} increased to 3.0 mol%, both the stimulation and emission maxima redshifted slightly, which is assumed to be due to increased Eu^{2+} crystalline sector breaking in the sites of Ca(2) [24], [25].

3. RESULTS AND DISCUSSION

The concentrations of green-emitting phosphor $\text{Ca}_2\text{SiO}_4:\text{Eu}^{2+}$ and yellow-emitting phosphor $\text{YAG}:\text{Ce}^{3+}$ reversed in Figure 2. The modification has two purposes: the first is to maintain the value of average CCTs, and the second is to alter the absorption and scattering of WLEDs with two phosphor layers. As a consequence, this impacts the WLEDs color quality and light intensity performance. The WLEDs' color quality is thus determined by the $\text{Ca}_2\text{SiO}_4:\text{Eu}^{2+}$ concentration chosen. When the $\text{Ca}_2\text{SiO}_4:\text{Eu}^{2+}$ ratio increased from 2% to 20% Wt., the concentration of phosphor $\text{YAG}:\text{Ce}^{3+}$ reduced so that the average value of CCTs is preserved. It is also true in the case that WLEDs have color temperatures ranging from 5600 K to 8500 K.

Figure 3 depicts the concentration of the green phosphor $\text{Ca}_2\text{SiO}_4:\text{Eu}^{2+}$ influence upon the WLEDs transmittance spectra. It is feasible to make a decision based on the manufacturer's specifications. WLEDs that demand good color fidelity can diminish luminous flux by a tiny amount. As shown in Figure 3, white light is the spectral region's synthesis. This diagram depicts a 5000 K spectrum. Clearly, the intensity trend increases with concentration $\text{Ca}_2\text{SiO}_4:\text{Eu}^{2+}$ in two sections of the light spectrum: 420-480 nm and 500-640 nm. The luminous flux's rise is obviously in the two-band emission spectrum. If the blue-light disputing in the WLEDs light increases, implying that the light disputing on the layer of phosphorous as well as on WLEDs will increase, favoring color uniformity. When $\text{Ca}_2\text{SiO}_4:\text{Eu}^{2+}$ is used, this is a significant outcome. The color homogeneity of the high-temperature remote phosphor structure, in particular, is challenging to control. This study found that $\text{Ca}_2\text{SiO}_4:\text{Eu}^{2+}$, at both low and high color temperatures (5600 K and 8500 K), can improve the color quality of WLEDs.

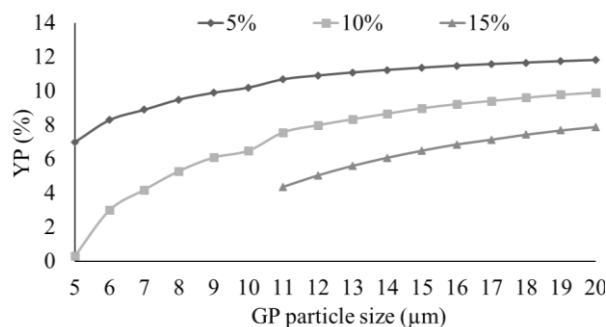


Figure 2. Maintaining the CCT average's value by changing phosphor's concentration

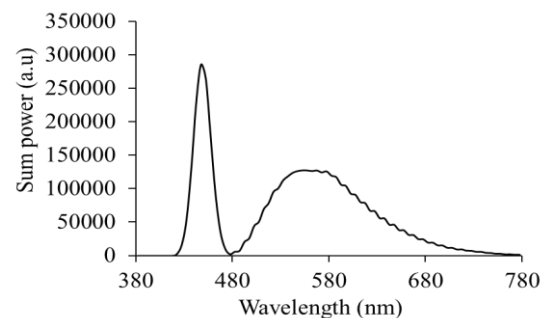


Figure 3. $\text{Ca}_2\text{SiO}_4:\text{Eu}^{2+}$ concentration functions as the emission spectra of 5000 K WLEDs

The paper demonstrated the efficiency of an emitted light flux on this double-layer distant layer of phosphor. The results in Figure 4 show that when the concentration of $\text{Ca}_2\text{SiO}_4:\text{Eu}^{2+}$ is increased from the value of 2% to 20% wt., the flux of light emitted increases dramatically. In all three average CCTs, the color divergence was significantly reduced with the concentration of phosphor $\text{Ca}_2\text{SiO}_4:\text{Eu}^{2+}$, which is demonstrated through Figure 5. The red phosphor layer's absorption is the reason for this. The LED chip's blue light was converted to green light when is absorbed by the $\text{Ca}_2\text{SiO}_4:\text{Eu}^{2+}$ phosphor. The yellow light is absorbed by the $\text{Ca}_2\text{SiO}_4:\text{Eu}^{2+}$ particles ignoring the LED chip's blue light. The LED chip's blue light absorption, however, is stronger than these two absorbs due to the material's absorption qualities. The addition of $\text{Ca}_2\text{SiO}_4:\text{Eu}^{2+}$ is a result of the rise of the WLEDs green elements, improving color uniformity index. In the present WLED lamp parameters, color homogeneity is amongst the most significant. The

greater the value of color homogeneity indice, the more expensive WLED white light is. However, the low cost of $\text{Ca}_2\text{SiO}_4:\text{Eu}^{2+}$ is an advantage. $\text{Ca}_2\text{SiO}_4:\text{Eu}^{2+}$ can thus be used in a variety of applications.

Color uniformity is only one criterion to consider when assessing WLED color quality. From a high color homogeneity indice, color quality cannot be considered good. Consequently, recent studies have developed terms which are called the color rendering indice and the color quality scale. When light shines on the color rendering index, it determines the object's natural color. The hue imbalance is caused by an excess of green light with the other primary colours of blue, yellow, and green. This has an impact on WLEDs' color quality, resulting in a decrease in color fidelity. In the inclusion of the distant CaAl sheet, the color rendering index CRI decreases slightly (Figure 6). Nonetheless, because CRI is merely a flaw in command-query separation CQS, these are allowed. When CRI and CQS are compared, CQS is more significant and more difficult to acquire. CQS is a three-factor index, with the first being the color rendering index, the second being the viewer's choice, the color coordination being the last index. The CQS is nearly a true gross assessment of the color quality for these crucial factors. Figure 7 shows an increase of the CQS in the presence of the distant phosphor $\text{Ca}_2\text{SiO}_4:\text{Eu}^{2+}$ layer. Furthermore, when the $\text{Ca}_2\text{SiO}_4:\text{Eu}^{2+}$ concentration is raised, CQS does not change considerably when the $\text{Ca}_2\text{SiO}_4:\text{Eu}^{2+}$ concentration is less than 10% wt. Both CRI and CQS are greatly diminished when $\text{Ca}_2\text{SiO}_4:\text{Eu}^{2+}$ concentrations are larger than 10% wt. due to severe color loss when green is dominant. As a result, when using green phosphor $\text{Ca}_2\text{SiO}_4:\text{Eu}^{2+}$, proper concentration selection is critical.

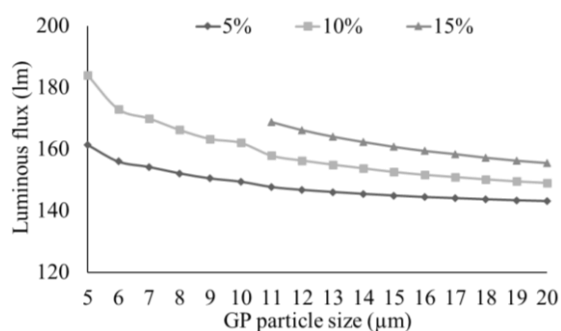


Figure 4. $\text{Ca}_2\text{SiO}_4:\text{Eu}^{2+}$ concentration functions as the luminous flux of WLEDs

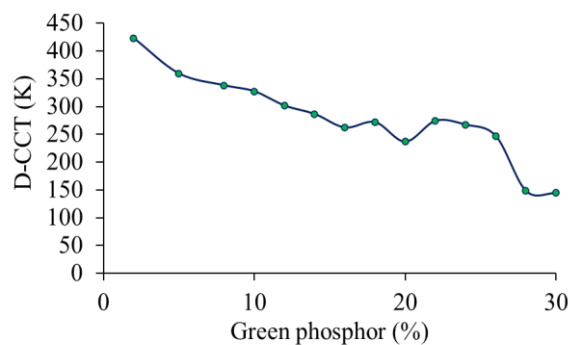


Figure 5. $\text{Ca}_2\text{SiO}_4:\text{Eu}^{2+}$ concentration functions as the color deviation of WLEDs

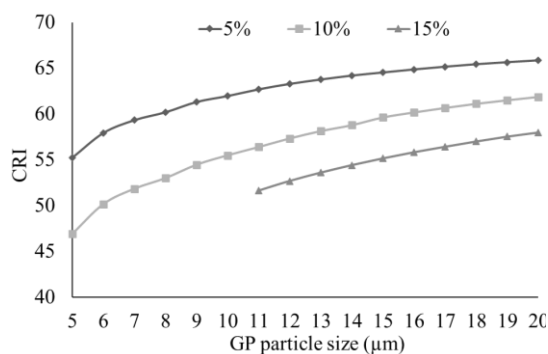


Figure 6. $\text{Ca}_2\text{SiO}_4:\text{Eu}^{2+}$ concentration functions as the color rendering index of WLEDs

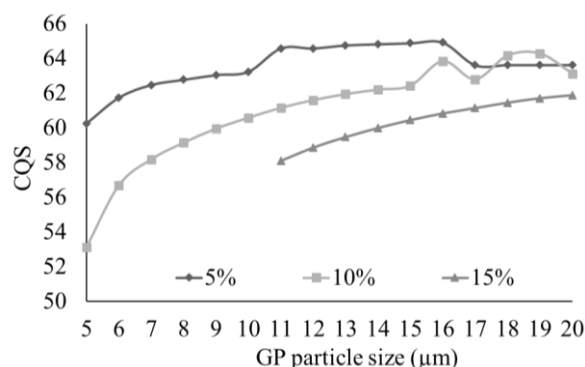


Figure 7. $\text{Ca}_2\text{SiO}_4:\text{Eu}^{2+}$ concentration functions as the color quality scale of WLEDs

4. CONCLUSION




Three independent production approaches (a traditional firm phase reaction (SSR) methodology, a fluid stage prototype technique employing SiO_2 sol (LPP- SiO_2 (sol)), and a liquid-based silicone combination (LPP-WSS)) were used to make green Eu^{2+} loaded Ca_2SiO_4 phosphors at various temperatures. The phosphors synthesized utilizing the three producing techniques displayed intense green illumination lay at the value of 502 nm and wide excitation spectra of 225 to 450 nm because of the $4f^7-4f^65d^1$ transition of Eu^{2+} .

After a thorough examination of the created phosphors, the LPP-WSS strategy was found to be the optimum way for synthesizing top-notch $\text{Ca}_2\text{SiO}_4:\text{Eu}^{2+}$ phosphors. For the phosphors manufactured utilizing the LPP-WSS process, the influence of the concentration of Eu^{2+} (0.1–5.0 mol percentage) was investigated as well. 3.0 mol percent was found to be the ideal concentration for maximal intensity. The $\text{Ca}_2\text{SiO}_4:\text{Eu}^{2+}$ phosphor made using the LPP-WSS approach showed a more uniform stage dispersion and greater luminous ferocity than others which




REFERENCES

- [1] G. Zhang, K. Ding, G. He and P. Zhong, "Spectral optimization of color temperature tunable white LEDs with red LEDs instead of phosphor for an excellent IES color fidelity index," *OSA Continuum*, vol. 2, pp. 1056-1064, 2019, doi: 10.1364/OSAC.2.001056.
- [2] X. Pan, D. Hou, M. Zhou, H. Lai, H. Ming and X. Ye, "HF-Free Preparation, High Thermal and Color Stability of Mn^{4+} -Activated K_2TiF_6 Red Phosphors for White Light-Emitting Diodes," *ECS Journal of Solid State Science and Technology*, vol. 7, no. 1, pp. 1-7, 2018, doi: 10.1149/2.0011801jss.
- [3] J. Silver, P. J. Marsh, G. R. Fern, T. G. Ireland and A. Salimian, "ZnCdS:Cu,Al,Cl: A Near Infra-Red Emissive Family of Phosphors for Marking, Coding, and Identification," *ECS Journal of Solid State Science and Technology*, vol. 7, pp. 1-8, 2018, doi: 10.1149/2.0131801jss.
- [4] X. Ma, S. Sun and J. Ma, "A novel orange-red $\text{Sr}_9\text{Ga}(\text{PO}_4)_7: \text{Sm}^{3+}$ phosphors for white light emitting diodes," *Material Research Express*, vol. 6, no. 11, pp. 116207, 2019, doi: 10.1088/2053-1591/ab47c6.
- [5] X. Zhang, R. Cui, J. Zhong, X. Qi and C. Deng, "A Novel Red-Emitting Phosphor $\text{Ca}_2\text{GdNbO}_6: \text{Eu}^{3+}$: Influences of Sintering Temperature and Eu^{3+} Concentration on the Photoluminescence," *ECS Journal of Solid State Science and Technology*, vol. 10, pp. 026003, 2021, doi: 10.1149/2162-8777/abed17.
- [6] K. Su, Q. Zhang, X. Yang and Bin Ma, "Crystal structure and luminescence properties of thermally stable Sm^{3+} -doped $\text{Sr}_9\text{In}(\text{PO}_4)_7$ orange-red phosphor," *Journal of Physics D: Applied Physics*, vol. 53, no. 38, pp. 385101, 2020, doi: 10.1364/OSAC.2.001056.
- [7] Y. V. Baklanova, L. G. Maksimova, O. A. Lipina, P. P. Tyutunnik, "A red-emitting phosphor based on Eu^{3+} -doped $\text{Li}_6\text{SrLa}_2\text{Ta}_2\text{O}_{12}$ garnets for solid state lighting applications," *Materials Research Express*, vol. 6, no. 6, pp. 066201, 2019, doi: 10.1088/2053-1591/ab093b.
- [8] G. Rahate, V. R. Panse, S. J. Dhoble, N. S. Kokode and K. Sharma, "Photoluminescence studies and synthesis of $\text{K}_2\text{SrPO}_4:\text{Ce}^{3+}, \text{Eu}^{3+}$ blue and orange-red emitting phosphor," *IOP Conference Series: Materials Science and Engineering*, vol. 1120, pp. 012005, 2021, doi: 10.1088/1757-899X/1120/1/012005.
- [9] S. Adachi, "Review—Tanabe—Sugano Energy-Level Diagram and Racah Parameters in Mn^{4+} -Activated Red and Deep Red-Emitting Phosphors," *ECS Journal of Solid State Science and Technology*, vol. 8, no. 12, pp. R183, 2019, doi: 10.1149/2.0281912jss.
- [10] L. Lei, Z. He, Z. Qun, Y. C. Feng, G. C. Chao and L. Yi, "Influences of sol-gel progress on luminescent properties of $\text{Li}_1.0\text{Nb}_0.6\text{Ti}_0.5\text{O}_3:\text{Eu}^{3+}$ red phosphor," *Materials Research Express*, vol. 6, no. 4, pp. 046202, 2019, doi: 10.1088/2053-1591/aaf91a.
- [11] C. He *et al.*, "Preparation and photoluminescence properties of red-emitting phosphor $\text{ZnAl}_2\text{O}_4:\text{Eu}^{3+}$ with an intense $5\text{D}_0 \rightarrow 7\text{F}_2$ transition," *Materials Research Express*, vol. 5, no. 2, pp. 025501, 2018, doi: 10.1088/2053-1591/aaa7c9.
- [12] O. M. ten Kate, Y. Zhao, K. M. B. Jansen, J. R. V. Ommen, "Effects of Surface Modification on Optical Properties and Thermal Stability of $\text{K}_2\text{SiF}_6:\text{Mn}^{4+}$ Red Phosphors by Deposition of an Ultrathin Al_2O_3 Layer Using Gas-Phase Deposition in a Fluidized Bed Reactor," *ECS Journal of Solid State Science and Technology*, vol. 8, no. 6, pp. R88, 2019, doi: 10.1149/2.0281906jss.
- [13] X. Yao, M. Cai and S. Man, "Preparation and Properties of Cr^{3+} Doped $\text{Mg}_0.388\text{Al}_2.408\text{O}_4$ Red Phosphor," *IOP Conference Series: Materials Science and Engineering*, vol. 782, pp. 022020, 2020, doi: 10.1088/1757-899X/782/2/022020.
- [14] Q. Wei, Z. Yang, Z. Z. Yang, Q. Zhou and Z. Wang, "Communication—Luminescent Properties of Mn^{4+} -Activated K_3HfF_7 Red Phosphor," *ECS Journal of Solid State Science and Technology*, vol. 7, no. 5, pp. R39, 2018, doi: 10.1149/2.0051805jss.
- [15] T. Pang and Z. Huanget, "A novel upconversion phosphor $\text{Gd}_2\text{Mo}_4\text{O}_{15}:\text{Yb}^{3+}, \text{Ho}^{3+}$: intense red emission and ratiometric temperature sensing under 980 nm excitation," *Materials Research Express*, vol. 5, no. 6, pp. 066204, 2018, doi: 10.1088/2053-1591/aacc8e.
- [16] Q. Wei, Z. Yang, Y. Liu, Q. Zhou and Z. Wang, "Communication—Highly Efficient Red-Emitting Phosphor $\text{Na}_2\text{SiF}_6:\text{Mn}^{4+}$ Prepared in H_3PO_4 Environment," *ECS Journal of Solid State Science and Technology*, vol. 9, no. 2, pp. 026004, 2020, doi: 10.1149/2162-8777/ab709b.
- [17] D. Shi *et al.*, "Communication—Luminescence Properties of a Novel $\text{Rb}_2\text{K}_2\text{GaF}_6:\text{Mn}^{4+}$ Red-Emitting Phosphor for Solid-State Lighting," *ECS Journal of Solid State Science and Technology*, vol. 9, no. 12, pp. 126001, 2020, doi: 10.1149/2162-8777/abc835.
- [18] N. Dhananjaya, S. R. Yashodha and C. Shikumarra, "The orange red luminescence and conductivity response of Eu^{3+} doped GdOF phosphor: synthesis, characterization and their Judd-Ofelt analysis," *Materials Research Express*, vol. 6, no. 12, pp. 1250a2, 2019, doi: 10.1088/2053-1591/ab4a6b.
- [19] Y. Masubuchi *et al.*, "Large red-shift of luminescence from $\text{BaCN}_2:\text{Eu}^{2+}$ red phosphor under high pressure," *Applied Physics Express*, vol. 13, no. 4, pp. 042009, 2020, doi: 10.35848/1882-0786/ab8055.
- [20] T. G. Lim, Y. N. Ahn, H. W. Park and J. S. Yoo, "Red-Shifted Absorption of a Mn^{4+} -Doped Germanate Phosphor by Crystal Distortion," *ECS Journal of Solid State Science and Technology*, vol. 7, no. 1, pp. R3189, 2018, doi: 10.1149/2.0241801jss.
- [21] R. Kobayashi, H. Tamura, "A New Host Compound of Aluminum Lithium Fluoride Oxide for Deep Red Phosphors Based on $\text{Mn}^{4+}, \text{Fe}^{3+}$, and Cr^{3+} ," *ECS Transactions*, vol. 88, pp. 225, 2019, doi: 10.1149/08801.0225ecst.
- [22] S. Sakurai, T. Nakamura and S. Adachi, "Synthesis and properties of $\text{Rb}_2\text{GeF}_6:\text{Mn}^{4+}$ red-emitting phosphors," *Japanese Journal of Applied Physics*, vol. 57, no. 2, pp. 022601, 2018, doi: 10.7567/JJAP.57.022601.
- [23] C. Wu *et al.*, "Phosphor-converted laser-diode-based white lighting module with high luminous flux and color rendering index," *Optica Publishing Group*, vol. 28, no. 13, pp. 19085-19096, 2020, doi: 10.1364/OE.393310.
- [24] G. E. Romanova, V. I. Batshev and A. S. Believe, "Design of an optical illumination system for a tunable source with acousto-optical filtering," *Journal of Optical Technology*, vol. 88, no. 2, pp. 66-71, 2021, doi: 10.1364/JOT.88.000066.
- [25] L. V. Labunets, A. B. Borzov and I. M. Akhmetov, "Regularized parametric model of the angular distribution of the brightness factor of a rough surface," *Journal of Optical Technology*, vol. 86, no. 10, pp. 618-626, 2019, doi: 10.1364/JOT.86.000618.

BIOGRAPHIES OF AUTHORS

Phuc Dang Huu    received a Physics Ph.D degree from the University of Science, Ho Chi Minh City, in 2018. Currently, He is Research Institute of Applied Technology, Thu Dau Mot University, Binh Duong Province, Vietnam. His research interests include simulation LEDs material, renewable energy. He can be contacted at email: danghuuphuc@tdmu.edu.vn.



Dieu An Nguyen Thi    received a master of Electrical Engineering, HCMC University of Technology and Education, Vietnam. Currently, she is a lecturer at the Faculty of Electrical Engineering Technology, Industrial University of Ho Chi Minh City, Viet Nam. Her research interests are Theoretical Physics and Mathematical Physics. She can be contacted at email: nguyenthidieuan@iuh.edu.vn.